Y. F. Hwang
Senior Research Associate,
Applied Research Laboratory,
Pennsylvania State University,
P.O. Box 30,
State College, PA 16804-0030

M. Kim

P. J. Zoccola

Naval Surface Warfare Center,
Carderock Division,
West Bethesda, MD 20817-5700

Acoustic Radiation by Point- or Line-Excited Laminated Plates

This paper presents an elasticity theory solution for computation of acoustic radiation by a point- or line-excited fluid-loaded laminated plate, which may consist of a stack of an arbitrary number of different isotropic material layers. A one-side water-loaded three-layer sandwich plate, which consists of a hard rubber core sandwiched between two steel plates of equal thickness, was used as an example of the laminated plates. The approximated equivalent sandwich plate solutions were compared with the elasticity theory solutions. These results show that the approximated solutions are, as expected, valid only at frequencies much lower than the coincidence frequency. The numerical result also shows that, even at about one-tenth of the coincidence frequency, the approximated solutions suffer substantial error. The differences between the dry-side- and the wet-side-excited radiated fields of a single-layer uniform plate and a sandwich plate were investigated and compared, and found to be significantly different at frequencies above the coincidence frequency. [S0739-3717(00)01803-1]

Introduction

The forced responses and acoustic radiation by a point- or line-excited fluid-loaded infinite plate have been investigated by authors such as Heckl [1], Thompson and Rattayya [2], Maidanik and Kerwin [3], Feit [4], Crighton and Innes [5], and many others, using either the classic thin plate or Timoshenko-Mindlin plate theory. It is well known that the classic thin plate theory is only applicable at frequencies much lower than the coincidence frequency. Using the Timoshenko-Mindlin plate theory has shown a considerable improvement of the classic theory, especially at and near the coincidence frequency [6]. Elasticity theory was used by Gur and Leehey [7] to solve for the far-field radiated sound pressure and the near-field displacement of an elastic plate, treated as a layer of elastic medium (slab), subject to a point- or line-force. From this analysis, they have discussed the upper frequency limit for the validity of the classic thin plate theory. Elasticity theory was also used by Pathak and Stepanishen [8] for acoustic radiation from a fluid-loaded infinite elastic plate subject to a general arbitrary loading, with numerical examples given for the far-field pressure patterns radiated from a plate driven by a line force at low, intermediate, and high frequencies. The above studies have facilitated both the approximated and exact solutions for acoustic radiation by a fluid-loaded single-layer uniform plate.

Due to the increased usage of multilayer composite systems in structural and noise control engineering, this paper addresses acoustic radiation by a point- or line-excited plate that may consist of a stack of an arbitrary number of different isotropic material layers. In order to have a wide variety of applications at a broad range of frequencies, elasticity theory is used. Each layer of the plate can be either very thin or very thick, i.e., the thickness of any layer can be larger than the characteristic wavelengths in the layer. Therefore, this method will be applicable to a laminated fiber-reinforced composite plate if both the fiber and matrix layers of the composite are, or are approximately, isotropic. Fluid on one side of the plate may be different from that on the other side, or one side may be a vacuum. In the case of a one-side water-loaded plate, elasticity theory allows one to assess the differences between the radiated pressure field caused by dry-side excitation and that caused by wet-side excitation. In the classic thin plate and Timoshenko-Mindlin plate theories, these differences cannot be distinguished. Because these theories involve the addition of fluid impedance to the plate impedance against the drive force, they are consistent with the elastic theory formulation in which force is placed on the wet side.

In light of the above arguments, the radiated pressure by a single-layer steel plate excited by a point-force placed on either the dry or wet side of the plate was calculated, and the results were compared with those of the classic thin plate and Timoshenko-Mindlin plate theories. In the wet-side drive result, where the comparison with the latter theories is relevant, the elasticity theory shows further improvement from the Timoshenko-Mindlin plate theory at the coincidence and higher frequencies. Below the coincidence frequency, there is no difference between the dry- and wet-side excitation. Above coincidence frequency, the radiated field produced by the dry-side excitation is stronger than that produced by the wet-side excitation, except at the resonance frequencies of the thickness-wise compressional modes. At those resonant peaks, the radiated field is independent of the side to which the force is applied. A one-side water-loaded three-layer sandwich plate, which consists of a hard rubber core sandwiched between two steel plates of equal thickness, was used as an example for the multilayer composite plates. An approximated equivalent sandwich plate solution [9] was compared to the elasticity theory solution. The result shows that the approximated solution is, as expected, only valid at frequencies much lower than the coincidence frequency. The differences between the dry-side- and the wet-side-excited radiated fields in a sandwich plate are much more pronounced than those in a single-layer plate. Contrary to that of a single-layer steel plate, the radiated field by a sandwich plate subject to the dry-side excitation is, in general, weaker than that subject to the wet-side excitation. This difference may be attributed to the isolation of the dry-side excitation provided by the softer rubber core, especially at frequencies above its fundamental thickness mode.

Mathematical Formalism

For computations of acoustic radiation from a multilayer plate, this study utilized a mathematical formalism derived from the well-known exact elasticity theory solution for the propagation of plane waves in a multilayer elastic system. This elasticity theory solution was first introduced by Thomson [10] and later described in detail in a textbook by Brekhovskikh [11], whose printed errors were later corrected in a paper by Folds and Loggins [12]. Many applications of this method followed: for example, Martin [13] and Jackins and Gaunaurd [14] used it to investigate the flow

Contributed by the Technical Committee on Vibration and Sound for publication in the JOURNAL OF VIBRATION AND ACOUSTICS. Manuscript received Nov. 1999; revised March 2000. Associate Technical Editor: R. L. Clark.

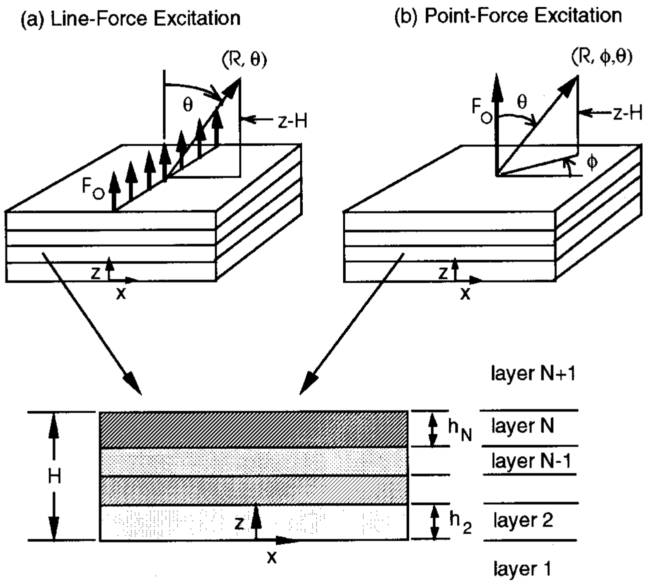

Fig. 1 A multilayer composite plate subject to a point- or line-force

noise reduction by an elastomeric layer and the resonance and acoustic scattering from stacks of bonded elastic plates, respectively.

This method (described in Refs. [10–12]) was intended for the analysis of sound transmission across and reflection from a multilayer media subject to an incident plane acoustic wave. This paper will briefly summarize the method and will then show how the method may be applied to the analysis of acoustic radiation from a multilayer composite plate subject to a line- or point-force excitation.

The multilayer system shown in Fig. 1 consists of N interfacial surfaces. It thus has $N-1$ finite layers (layer 2 through layer N) of various materials, with two semi-infinite fluid media on both sides of the plate, labeled as the 1st and $(N+1)$th layer. All interfaces are in the x-y plane and of infinite extent. Stresses and velocities of plane harmonic waves in any layer, say the nth layer, can be deduced from the following potential functions:

$$\left.\begin{aligned}\varphi_n&=(A_n e^{i\alpha_n z}+B_n e^{-i\alpha_n z})e^{i(kx-\omega t)}\\ \psi_n&=(C_n e^{i\beta_n z}+D_n e^{-i\beta_n z})e^{i(kx-\omega t)}\end{aligned}\right\} \tag{1}$$

where φ and ψ are the dilatational and shear wave potentials; $(\alpha_n=[\omega^2/(c^2_{(l,n)}(1-i\eta_l)-k^2)]^{1/2}$ and $\beta_n=[\omega^2/(c^2_{(s,n)}(1-i\eta_s)-k^2)]^{1/2}$, $c_{(l,n)}$ and $c_{(s,n)}$, and η_l and η_s, are their corresponding z-coordinate propagating constants, wave speeds, and loss factors, respectively. The wave number, k, is obviously the x-component propagating constant shared by all propagating waves. The origin of the coordinates in Eq. (1) may be located at the lower surface of the layer (at the interface between layers n and $n-1$). Velocities (v) and stresses (Z) can be obtained from the potential functions by differentiation; i.e.,

$$\begin{Bmatrix} v_x^n\\ v_z^n\\ Z_z^n\\ Z_x^n\end{Bmatrix}=\begin{bmatrix}\dfrac{\partial}{\partial x} & -\dfrac{\partial}{\partial z}\\ \dfrac{\partial}{\partial z} & \dfrac{\partial}{\partial x}\\ \dfrac{i}{\omega}\left(\lambda\dfrac{\partial^2}{\partial x^2}+(\lambda+2\mu)\dfrac{\partial^2}{\partial z^2}\right) & \dfrac{2\mu i}{\omega}\dfrac{\partial^2}{\partial x\partial z}\\ \dfrac{\mu i}{\omega}\dfrac{\partial^2}{\partial x^2} & \dfrac{\mu i}{\omega}\dfrac{\partial^2}{\partial z^2}\end{bmatrix}\begin{Bmatrix}\varphi_n\\ \psi_n\end{Bmatrix} \tag{2}$$

where λ and μ are the Lame' constants. The values of $v_x^n v_z^n Z_z^n Z_x^n$ at the upper boundary, $z=h_n$ (thickness of the nth layer), can be expressed in terms of $A_nB_nC_nD_n$ by substitutions of Eq. (1) into Eq. (2). Similarly, at the lower boundary, the values of $v_x^{n-1}v_z^{n-1}Z_z^{n-1}Z_x^{n-1}$ can also be expressed in terms $A_nB_nC_n$ and D_n when evaluated at $z=0$. Eliminating $A_nB_nC_n$ and D_n by some algebraic manipulations, the relationship of velocity and stress between the two bounding surfaces of the nth layer can be established as follows:

$$\begin{Bmatrix} v_x^n\\ v_z^n\\ Z_z^n\\ Z_x^n\end{Bmatrix}=\begin{bmatrix} a_{11}^n & a_{12}^n & a_{13}^n & a_{14}^n\\ a_{21}^n & a_{22}^n & a_{23}^n & a_{24}^n\\ a_{31}^n & a_{32}^n & a_{33}^n & a_{34}^n\\ a_{41}^n & a_{42}^n & a_{43}^n & a_{44}^n\end{bmatrix}\begin{Bmatrix} v_x^{n-1}\\ v_z^{n-1}\\ Z_z^{n-1}\\ Z_x^{n-1}\end{Bmatrix} \tag{3}$$

The formula for the coefficients, a_{ij}^n, of matrix A^n that depend on the physical and geometrical properties of the layer are given in Ref. [12] and will not be repeated here. It can be easily shown that Eq. (3) is independent of the location of the coordinate origin. This independence, along with the enforcement of continuity of displacements (or particle velocity) and stresses at all interfaces, allows us to establish the relationship between the Nth and the 1st interfaces by successive multiplication of A^n, for $n=2,3,\ldots,N$; i.e.,

$$\begin{Bmatrix} v_x^N\\ v_z^N\\ Z_z^N\\ Z_x^N\end{Bmatrix}=\begin{bmatrix} A_{11} & A_{12} & A_{13} & A_{14}\\ A_{21} & A_{22} & A_{23} & A_{24}\\ A_{31} & A_{32} & A_{33} & A_{34}\\ A_{41} & A_{42} & A_{43} & A_{44}\end{bmatrix}\begin{Bmatrix} v_x^1\\ v_z^1\\ Z_z^1\\ Z_x^1\end{Bmatrix} \tag{4}$$

where $A=A^NA^{N-1}\ldots A^n\ldots A^3A^2$. Note that the superscripts $(n=2,3,\ldots)$ shown above are indices rather than exponents of the matrices.

Thus, in a given multilayer system at a given frequency, Eq. (4) relates velocities and stresses on the two outer surfaces as a function of k. When layers 1 and $N+1$ are inviscid fluids, the shear stresses Z_x^1 and Z_x^N must be zero. Using these conditions with some substitutions, Eq. (4) may be reduced to

$$\begin{Bmatrix} v_z^N\\ Z_z^N\end{Bmatrix}=\begin{bmatrix} M_{22} & M_{23}\\ M_{32} & M_{33}\end{bmatrix}\begin{Bmatrix} v_z^1\\ Z_z^1\end{Bmatrix} \tag{5}$$

where

$$M_{22}=A_{22}-A_{21}A_{42}/A_{41},\quad M_{23}=A_{23}-A_{21}A_{43}/A_{41}$$

$$M_{32}=A_{32}-A_{31}A_{42}/A_{41},\quad M_{33}=A_{33}-A_{31}A_{43}/A_{41}$$

Equation (5) was used in Refs. [11] and [12] to derive the reflection and transmission coefficients of a multilayer plate subject to an incident plane wave in the upper fluid medium (the $N+1$th layer). Note that the dependence of k and ω of the above variables is suppressed for clarity.

Radiation from a Line-Force Excitation

A line harmonic force of root-mean-square amplitude F_0 units per linear length along the y-axis may be represented as a distribution in x by $F_0\delta(x)e^{-i\omega t}$, where $\delta(x)$ is the Dirac delta function. This line force is assumed to be applied on the outer surface (the interface between the Nth layer and the $N+1$th semi-infinite fluid space) of the multilayer system. Let $Z_F(k)$ be the spatial Fourier transform of the line force; then

$$F_0\delta(x)e^{-i\omega t}=\frac{1}{2\pi}\int_{-\infty}^{\infty}Z_F(k)e^{i(kx-\omega t)}dk,\quad \text{and}\quad Z_F(k)=Fo \tag{6}$$

Since the term, $F_0\delta(x)$, has the dimension of force per unit area (stress), $Z_F(k)e^{i(kx-\omega t)}$ must have the dimension of stress per wave number. Using $Z_F(k)e^{i(kx-\omega t)}$ as the forcing function is therefore compatible with Eqs. (1–5).

When the exterior fluids, the upper and lower fluid half spaces (the $N+1$th and 1st layer) are present, their corresponding specific impedances as a function of k and ω are

$$\zeta_1=\rho_1\omega/\sqrt{(k_0^1)^2-k^2}, \quad \zeta_{N+1}=\rho_{N+1}\omega/\sqrt{(k_0^{N+1})^2-k^2} \quad (7)$$

where $k_0^i=\omega/c_i$, ρ_i and c_i $(i=1, N+1)$ are the sonic wave number, fluid density and speed of sound, respectively. Using Eqs. (5) and (7), we find the total impedance (solid and fluid impedances) at the drive surface to be $(M_{32}+\zeta_1 M_{33})/(M_{22}+\zeta_1 M_{23})+\zeta_{N+1}$. It follows that the drive surface and the transferred velocity responses per unit force, u_z^N and u_z^1, are

$$u_z^N=\frac{v_z^N}{F_0}=\frac{-(M_{22}+\zeta_1 M_{23})}{(M_{32}+\zeta_1 M_{33})+\zeta_{N+1}(M_{22}+\zeta_1 M_{23})} \quad (8)$$

and

$$u_z^1=\frac{v_z^1}{F_0}=\frac{-1}{(M_{32}+\zeta_1 M_{33})+\zeta_{N+1}(M_{22}+\zeta_1 M_{23})} \quad (9)$$

respectively. When there is no fluid on one or both sides of the plate, either ζ_1 or ζ_{N+1} or both of them must be zero. Once the two outer surface velocities are known, the radiated pressure fields at a given frequency, ω, in the upper- and lower-half fluid spaces are obviously

$$\frac{p^{N+1}(x,z)}{F_0}=\frac{\rho_{N+1}\omega}{2\pi}\int_{-\infty}^{\infty}\frac{u_z^N}{\alpha^{N+1}}e^{i(kx+\alpha_{N+1}(z-H))}dk \quad (10)$$

and

$$\frac{p^1(x,z)}{F_0}=-\frac{\rho_1\omega}{2\pi}\int_{-\infty}^{\infty}\frac{u_z^1}{\alpha^1}e^{i(kx-\alpha_1 z)}dk \quad (11)$$

where H is the total thickness of solid layers, $\alpha_i=\sqrt{(k_0^i)^2-k^2}$; $i=1, N+1$.

In a multilayer system, the variables u_z^N and u_z^1 in the above integrands are too complicated to be handled analytically. Equations (10) and (11) are numerically integrable as long as the poles of the integrands do not lie on the real axis, which is possible if non-zero loss factors for the fluid and solid layers are given. The far-field solutions of the above equations at (R,θ) can be obtained by the stationary-phase integration method [6], i.e.,

$$\frac{p^{N+1}(R,\theta)}{F_0}=\frac{\rho_{N+1}\omega}{\sqrt{2\pi k_0^{N+1}R}}u_z^N(k_0^{N+1}\sin\theta)e^{i(k_0^{N+1}R-\pi/4)} \quad (12)$$

and

$$\frac{p^1(R,\theta)}{F_0}=\frac{\rho_1\omega}{\sqrt{2\pi k_0^1 R}}u_z^1(k_0^1\sin\theta)e^{i(k_0^1 R-\pi/4)} \quad (13)$$

where $u_z^1(k_0^1\sin\theta)$ and $u_z^N(k_0^{N+1}\sin\theta)$ are the values of u_z^1 and u_z^N evaluated at k equals to $k_0^1\sin\theta$ and $k_0^{N+1}\sin\theta$, respectively. The radiated sound powers into the $N+1$th and 1st fluid media, $\Pi_{N+1}(\omega)$ and $\Pi_1(\omega)$, respectively, are then determined by evaluating

$$\frac{\Pi_{N+1}(\omega)}{F_0}=\frac{\rho_{N+1}\omega}{2\pi}\int_{-k_0^{N+1}}^{k_0^{N+1}}\frac{|u_z^N|^2}{\alpha^{N+1}}dk \quad (14)$$

and

$$\frac{\Pi_1(\omega)}{F_0}=\frac{\rho_1\omega}{2\pi}\int_{-k_0^1}^{k_0^1}\frac{|u_z^1|^2}{\alpha^1}dk \quad (15)$$

Again, these radiated powers must be obtained by performing the numerical integration along the real axis.

Radiation by a Point-Force Excitation

A point harmonic force of the root-mean-square amplitude F_0 may be represented by, $F_0\delta(x)\delta(y)e^{-i\omega t}$, which shows a distribution of the force in the x-y plane. Taking the 2-D spatial Fourier transform of this point force yields

$$\mathbf{Z}_F(k_x,k_y)=F_0 \quad (16)$$

where $\mathbf{Z}_F(k_x,k_y)$ is the transformed point-force that has the dimension of stresses as a function of wave vector, (k_x,k_y). In this case, the potentials of the wave functions in any layer, φ_n and ψ_n, and the exterior surface velocities per unit point force, $u_z^N(k_x,k_y,\omega)$ and $u_z^1(k_x,k_y,\omega)$, can be described using the previous corresponding equations by simply replacing (kx) and (k^2) with $(k_x x+k_y y)$ and $(k_x^2+k_y^2)$, respectively. The z-direction propagation factors that were a function of k^2 in Eq. (1) are now a function of $\gamma^2=(k_x^2+k_y^2)$, i.e.,

$$\alpha_n=\left[\frac{\omega^2}{c_{(l,n)}^2(1-i\eta_l)}-\gamma^2\right]^{1/2}$$

and

$$\beta_n=\left[\frac{\omega^2}{c_{(s,n)}^2(1-i\eta_s)}-\gamma^2\right]^{1/2}.$$

Similar to Eqs. (10) and (11), the radiated pressure fields on the upper and lower media are

$$\frac{p^{N+1}(x,y,z)}{F_0}=\frac{1}{(2\pi)^2}\int_{-\infty}^{\infty}\zeta_{N+1}(k_x,k_y,\omega)u_z^N(k_x,k_y,\omega)\times e^{i(k_x x+k_y y+\alpha_{N+1}(z-H))}dk_x dk_y \quad (17)$$

and

$$\frac{p^1(x,y,z)}{F_0}=\frac{1}{(2\pi)^2}\int_{-\infty}^{\infty}\zeta_1(k_x,k_y,\omega)u_z^1(k_x,k_y,\omega)\times e^{i(k_x x+k_y y-\alpha_1 z)}dk_x dk_y \quad (18)$$

respectively, where $\zeta_1=\rho_1\omega/\sqrt{(k_0^1)^2-\gamma^2}$, $\zeta_{N+1}=\rho_{N+1}\omega/\sqrt{(k_0^{N+1})^2-\gamma^2}$. The pressure field induced by a point-force is more conveniently expressed in the cylindrical coordinates (r,ϕ,z). Since the field has no angular dependency on ϕ in the x-y plane, the radiated pressure field that is transformed into the cylindrical coordinates becomes

$$\frac{p^{N+1}(r,z)}{F_0}=\frac{\rho_{N+1}\omega}{2\pi}\int_0^{\infty}\frac{u_z^{N+1}(\gamma,\omega)}{\sqrt{(k_0^{N+1})^2-\gamma^2}}\times e^{i\sqrt{(k_0^{N+1})^2-\gamma^2}(z-H)}J_0(\gamma r)\gamma d\gamma \quad (19)$$

and

$$\frac{p^1(r,z)}{F_0}=\frac{\rho_1\omega}{2\pi}\int_0^{\infty}\frac{u_z^1(\gamma,\omega)}{\sqrt{(k_0^1)^2-\gamma^2}}e^{-i\sqrt{(k_0^1)^2-\gamma^2}z}J_0(\gamma r)\gamma d\gamma \quad (20)$$

Following the procedure of the stationary-phase method described by Junger and Feit [6], we obtain the following far-field solutions:

$$\frac{p^{N+1}(R,\theta)}{F_0}=\frac{i\rho_{N+1}\omega e^{ik_0^{N+1}R}}{2\pi R}u_z^N(k_0^{N+1}\sin\theta) \quad (21)$$

and

$$\frac{p^1(R,\theta)}{F_0}=\frac{i\rho_1\omega e^{ik_0^1 R}}{2\pi R}u_z^1(k_0^1\sin\theta) \quad (22)$$

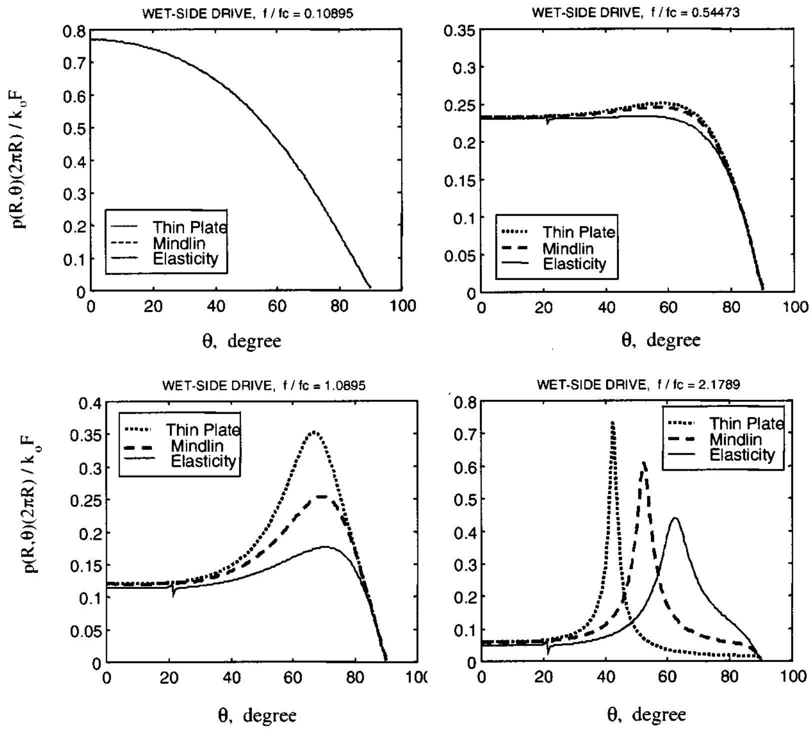

Fig. 2 Radiated pressures by a uniform plate subjected to a wet-side point-force

Since the laminated plate is homogeneous in the (x,y) plane, $u_z^1(\gamma)$ and $u_z^N(\gamma)$ are independent of the polar angle, ϕ, and they may be evaluated, without loss of generality, along the x-axis where $k_y=0$ and $\gamma=k_x=k$. Therefore, $u_z^1(\gamma)$ and $u_z^N(\gamma)$ can be evaluated directly from Eqs. (8) and (9), respectively.

Similar to the case of a line excitation, the sound powers radiated into the 1st and $N+1$th fluid media, $\Pi_1(\omega)$ and $\Pi_{N+1}(\omega)$, respectively, are

$$\frac{\Pi_{N+1}(\omega)}{F_0}=\frac{1}{2\pi}\int_{-k_0^{N+1}}^{k_0^{N+1}}\frac{|u_z^{N+1}(\gamma,\omega)|^2}{\zeta_{N+1}(\gamma,\omega)}\gamma d\gamma \tag{23}$$

and

$$\frac{\Pi_1(\omega)}{F_0}=\frac{1}{2\pi}\int_{-k_0^1}^{k_0^1}\frac{|u_z^1(\gamma,\omega)|^2}{\zeta_1(\gamma,\omega)}\gamma d\gamma \tag{24}$$

As discussed earlier, as long as loss factors for any of the materials are not zero, Eqs. (23) and (24) are numerically integrable because the poles of $u_z^1(\gamma)$ and $u_z^N(\gamma)$ will not occur on the real axis.

Numerical Examples

The above equations for computing radiated power and pressure fields are applicable to the following combinations of fluid media on both sides of the plate: (1) both sides loaded with heavy fluid such as water, (2) both sides loaded with light fluid such as air, (3) one side with heavy fluid but the other with light fluid, and (4) one side with fluid while the other is a vacuum (the latter will be the dry side, with zero fluid impedance, if the other side is water). The force of excitation in the last case may be placed on either the dry- or wet-side of the plate. Since the drive force is always placed on the Nth surface, the $N+1$th layer must be a vacuum in the case of dry-side excitation; similarly, the first layer must be a vacuum in the case of wet-side excitation. This elasticity theory formulation thus allows one to assess the differences between the radiated pressure field caused by the dry-side excitation and that caused by the wet-side excitation. When using the classic thin plate and Timoshenko-Mindlin plate theories, these differences cannot be distinguished.

In the plate theories (thin and Timoshenko-Mindlin plates), fluid impedance is added to the plate impedance against the drive force. This classic approach is consequently consistent with the elastic theory formulation, in which force is placed on the wet side. In light of the above arguments, the radiated pressure by a single-layer (5 cm) steel plate excited by a point-force placed on either the dry- or wet-side of the plate is calculated, and the results are compared with those of the classic thin plate and Timoshenko-Mindlin plate theories (calculated using the formula presented in

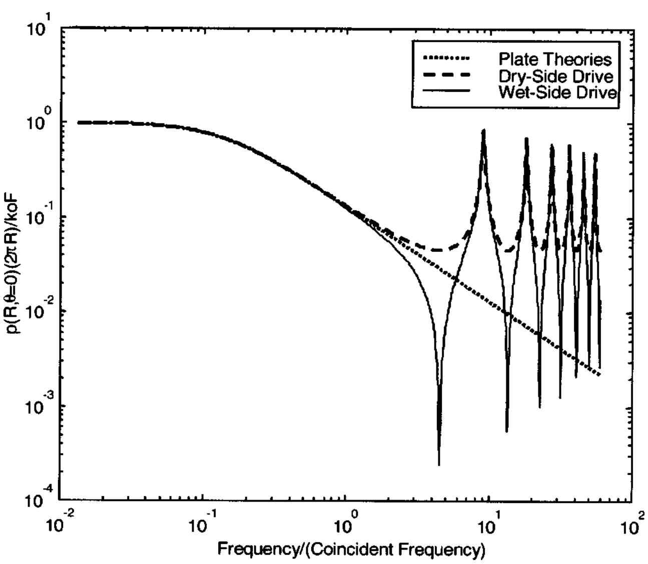

Fig. 3 Radiated pressures by a uniform plate subjected to a wet-side point-force, at $\theta=0$

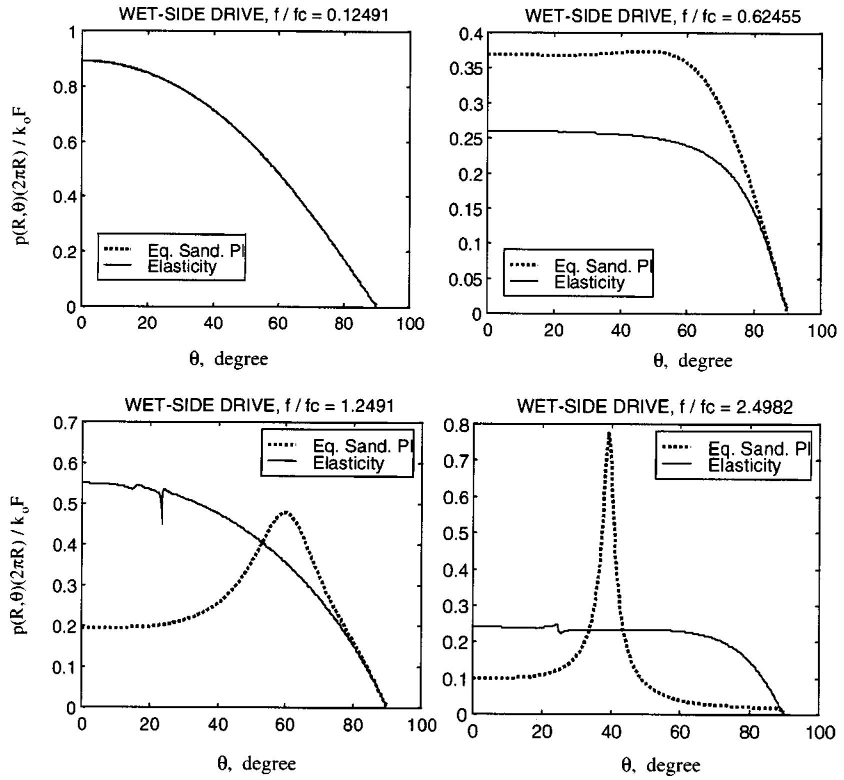

Fig. 4 Radiated pressures by a sandwich plate subjected to a wet-side point-force

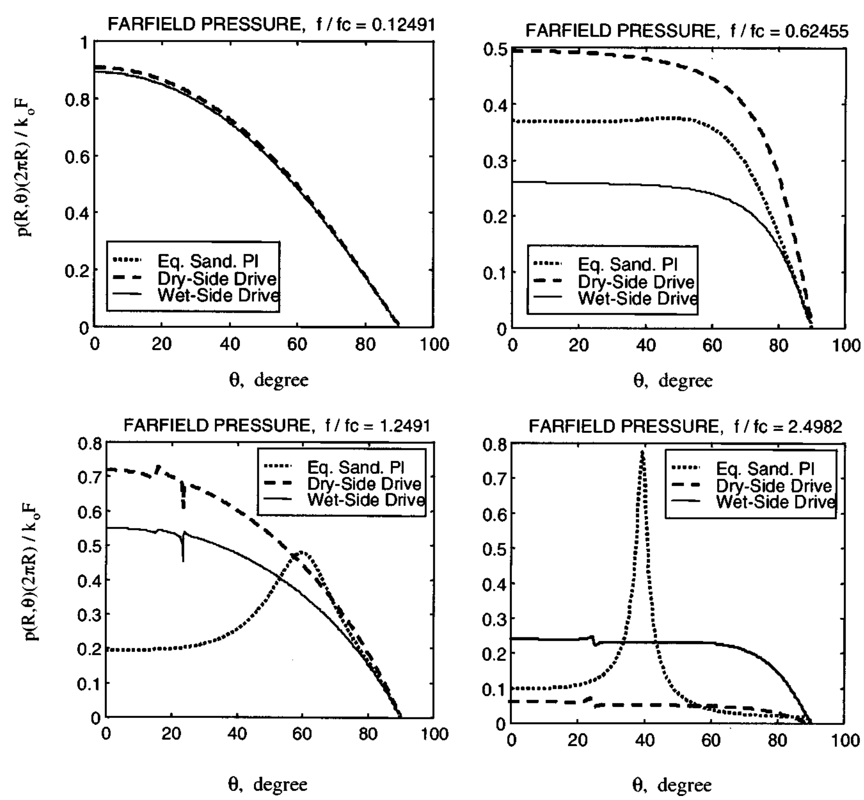

Fig. 5 Radiated pressures by a sandwich plate subjected to a dry- or wet-side point-force

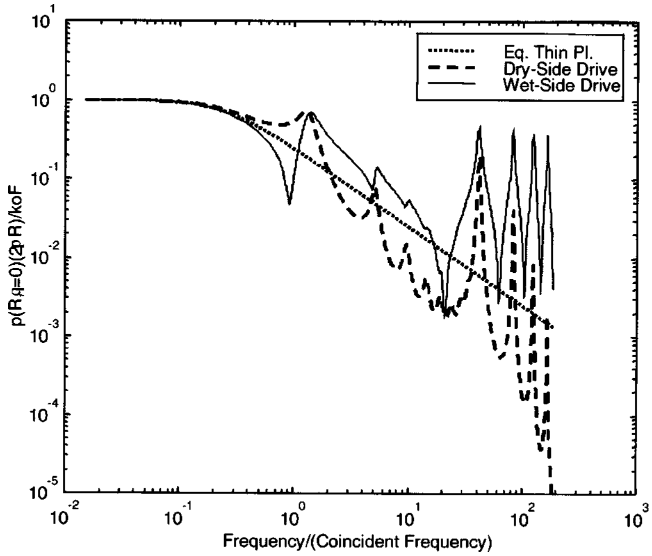

Fig. 6 Broadside radiated pressures by a sandwich plate subjected to a dry- or wet-side point-force

Ref. [6]). The loss factor of steel is assumed to be 0.005 in these calculations. Figure 2 shows the normalized far-field pressure, $p(R,\theta)(2\pi R)/k_0F_0$, subject to a wet-side point-excitation at various normalized frequencies, f/f_c, where f_c is the coincidence frequency of the plate. At frequencies much below the coincidence frequency, say $f/f_c \sim 0.1$, there is no difference which theory is used. This figure also shows the differences between the result of the thin plate theory and that of the exact elasticity theory at higher frequencies. As expected, the result from Timoshenko-Mindlin theory (which is a substantially improved theory from the thin plate theory) lies between the two.

The differences in $p(R,\theta)(2\pi R)/k_0F_0$ (when $\theta=0$) between the dry- and wet-side excitation of a uniform steel plate are demonstrated in Fig. 3, which shows that above the coincidence frequency, the radiated field produced by the dry-side excitation is stronger than that produced by the wet-side excitation, except at the resonance frequencies of the thickness-wise modes associated with the compressional waves. At those resonant peaks, the radiated field is independent of the side to which force is applied. The smoother curve shown (as a dotted line) in this figure is calculated from the thin plate theory which basically cannot tell which side the force is applied.

A one-side water-loaded three-layer sandwich plate, which consists of a 3.8 cm hard rubber core (physical properties shown in Ref. [15], loss factor=0.1 assumed) sandwiched between two steel plates of equal thickness (1.8 cm), was used as an example of the multilayer composite plates. Figure 4 shows $p(R,\theta)(2\pi R)/k_0F_0$ calculated from the elasticity theory solution subject to the wet-side excitation and that from the approximated equivalent sandwich plate solution [9]. The equivalent sandwich plate solution is essentially a classic thin plate solution using the equivalent bending rigidity of the sandwich plate (Eqs. (2.2) and (2.3) of Ref. [9]). This comparison shows, as expected, that the approximated solution is only valid at frequencies substantially below the coincidence frequency. The differences between the dry-side- and wet-side-excited radiated fields in a sandwich plate are also shown in Fig. 5. These differences are much more pronounced than those in a single-layer steel plate. Figure 6 shows similar comparisons for $p(R,\theta)(2\pi R)/k_0F_0$, except that the curves shown are plotted as a function of f/f_c for $\theta=0$. Contrary to that of a single-layer steel plate (shown in Fig. 3), the broadside radiated field by a sandwich plate subject to dry-side excitation is, in general, weaker than that plate subject to wet-side excitation. This difference may be attributed to the isolation of the dry-side excitation provided by the softer rubber core, especially at frequencies above its fundamental thickness mode.

Conclusion and Future Work

This paper has presented an elasticity theory solution for computation of acoustic radiation by a point- or line-excited fluid-loaded thin or thick composite plate, which may consist of a stack of an arbitrary number of different isotropic material layers or just a single layer uniform plate. The formulation allows for different fluids on both sides of the plate, and either side may be a vacuum. In the case of a one-side water-loaded plate, the elasticity theory allows one to assess the differences between the radiated pressure field caused by dry-side excitation and that caused by wet-side excitation. In the classic thin plate and Timoshenko-Mindlin plate theories, these differences cannot be distinguished. The radiated pressure field produced by a single-layer steel plate excited by a point-force placed on either the dry or wet side of the plate was calculated, and the results show a further improvement from the Timoshenko-Mindlin plate theory at the coincidence and higher frequencies. Above the coincidence frequency, the radiated field produced by the dry-side excitation is different from that produced by the wet-side excitation.

A one-side water-loaded three-layer sandwich plate, which consists of a hard rubber core sandwiched between two steel plates of equal thickness, was used as an example of the multilayer composite plates. Comparison of this result and that obtained from the approximated equivalent thin plate solution indicates that the approximated solutions are, as expected, valid only at frequencies substantially lower than the coincidence frequency. The numerical example shows that the approximated solutions suffer substantial error even at about one-tenth of the coincidence frequency. Also, the differences of the radiated fields between the dry- and wet-side excitation in a sandwich plate are much more pronounced than those in a single-layer plate. Therefore, the methodology shown in this paper is recommended for analysis of acoustic radiation by point- or line-excited laminated plates.

The method presented in this paper will be applicable to a laminated fiber-reinforced composite plate if both the fiber and matrix layers of the composite are, or are approximately, isotropic. The fiber layers are, however, mostly orthotropic or anisotropic. Therefore, an extension of this method to accommodate the orthotropic and, perhaps, more general anisotropic material layers are planned for a future work.

Acknowledgment

This work was supported by funding from Office of Naval Research, Code 334, and administered by Dr. Geoffrey L. Main, under the 6.2 Structural Acoustics Program (1993-1998) while the first author was employed at the Naval Surface Warfare Center, Carderock Division, West Bethesda, MD.

References

[1] Heckl, M., 1959, ''Sound Radiation by Point-Excited Plates,'' Acoustica, **9**, pp. 371–380.
[2] Thompson, Jr., W., and Rattayya, J. V., 1964, ''Acoustic Power Radiated by an Infinite Plate Excited by a Concentrated Moment,'' J. Acoust. Soc. Am., **36**, pp. 1488–1490.
[3] Maidanik, G., and Kerwin, Jr., E. M., 1966, ''Influence of Fluid Loading on the Radiation from Infinite Plate below the Critical Frequency,'' J. Acoust. Soc. Am., **40**, No. 5, pp. 1034–1038.
[4] Feit, D., 1966, ''Pressure Radiated by a Point-Excited Elastic Plate,'' J. Acoust. Soc. Am., **40**, pp. 1489–1494.
[5] Crighton, D. G., and Innes, D., 1983, ''Low-Frequency Acoustic Radiation and Vibration Response of Locally Excited Fluid Loaded Structures,'' J. Sound Vib., **91**, pp. 293–314.
[6] Junger, M. C., and Feit, D., 1993, *Sound, Structures, and Their Interactions*, Acoustical Society of America, American Institute of Physics.
[7] Gur, Y., and Leehey, P., 1992, ''Fluid-Loaded Elastic Slab Excited by Line and Point Loads,'' J. Acoust. Soc. Am., **92**, No. 4, Pt. 2, p. 2460.

[8] Pathak, A. G., and Stepanishen, P. R., 1993, ''Acoustic Harmonic Radiation from Fluid-Loaded Elastic Plates Using Elastic Theory,'' J. Acoust. Soc. Am., **94**, No. 3, Pt. 1, pp. 1700–1710.
[9] Nilsson, A. C., 1990, ''Wave Propagation in and Sound Transmission through a Sandwich Plate,'' J. Sound Vib., **138**, No. 1, pp. 73–94.
[10] Thomson, W., 1950, ''Transmission of Elastic Waves through a Stratified Medium,'' J. Appl. Phys., **21**, pp. 89–93.
[11] Brekhovskikh, L. M., 1960, *Waves in Layered Media*, Academic, New York.
[12] Folds, D. L., and Loggins, C. D., 1977, ''Transmission and Reflection of Ultrasonic Waves in Layered Media,'' J. Acoust. Soc. Am., **62**, No. 5, pp. 1102–1109.
[13] Martin, N. C., 1993, ''Fundamentals of Outer Decoupler Design for Flow Noise Reduction,'' J. Acoust. Soc. Am., **93**, No. 4, Pt. 2, p. 2287.
[14] Jackins, P. D., and Gaunaurd, G. C., 1986, ''Resonance and Acoustic Scattering from Stacks of Bonded Elastic Plates,'' J. Acoust. Soc. Am., **80**, No. 6, pp. 1762–1776.
[15] Kinsler, L. E., Frey, A. R., Coppens, A. B., and Sanders, J. V., 1982, *Fundamentals of Acoustics*, 3rd ed., Wiley, New York.